Mem. S.A.It. Suppl. Vol. 16, 141

Memorie della
Supplementi

Study of iron nanophases in ordinary chondrites by means of near field microscopy

A. Longobardo[1,2], E. Palomba[1], M. Girasole[3], G. Longo[3], G. Pompeo[3], P. Gori[3], and A. Cricenti[3]

[1] IFSI-INAF, Via Fosso del Cavaliere 100, 00133, Roma, Italy
e-mail: andrea.longobardo@ifsi-roma.inaf.it
[2] Dipartimento di Fisica, Università Sapienza, Piazzale Aldo Moro 5, 00185, Roma, Italy
[3] IMM-CNR, Via Fosso del Cavaliere 100, 00133, Roma, Italy

Abstract. The aim of this work is to study the role, the characteristics and the formation process of iron nanoparticles (npFe) in asteroids. These npFe are considered the main responsible for the reddening (i.e. red-IR reflectance increase at increasing wavelength) observed in the asteroids' spectra and it is believed that they are formed as consequence of the Space Weathering (i.e. the ensemble of processes acting on a body exposed to space environment). Moretti et al. (2005) discusses a scenario regarding npFe formation, according to which they originate from shock-induced phase transformations of Fe-Ni alloys caused by collisions.
We looked for npFe in samples of Ordinary Chondrites (OCs), whose parent bodies are S-type asteroids, and are trying to link the amount of metal and the mechanical shock degree (which would confirm the scenario above mentioned). For this purpose, we have choosen to use SNOM (Scanning Near-field Optical Microscopy). This technique permits to collect at the same time high resolution topography images and optical images of the analyzed sample.
For the first time, a multi-colour SNOM experiment (i.e. every sample has been analyzed at different wavelengths) has been performed on extraterrestrial samples: because npFe are more reflective at longer wavelengths, comparison of reflectance images obtained at different wavelength gives a strong aid in npFe detection and identification. Finally, laboratory analysis has been supported by simulation methods.

Key words. iron nanoparticles – Ordinary Chondrites – reddening – space weathering – near-field – SNOM

1. Introduction

Space weathering (SW) is an ensemble of processes that act on a body exposed to space environment. Development and accumulation of iron nanoparticles (npFe) on asteroid surfaces is a SW effect: this is evidenced by the fact that the asteroids reddening (i.e. the increase of IR reflectance with increasing wavelength), mainly due to npFe (Pieters et al. 2000), is more evident in asteroids than in meteorites. Space weathering processes that could lead to npFe formation are solar wind sputtering (Sasaki et al. 2001) and shock-induced phase transformation of Fe-Ni alloys caused by collisions (Moretti et al. 2005).

Our study is focused on analysis of Ordinary Chondrites (OCs), whose parent bodies are very probably S-type asteroids (Gaffey 1976; Bell et al. 1992), the most affected by the reddening (Sasaki et al. 2001). Hence a laboratory experiment, i.e. spectral analysis and nanoimaging of Ordinary Chondrite samples with different metallic content and shock degree, supported by simulation techniques, has been performed to clarify the role, the characteristics and the formation process of npFe in asteroids.

2. The SNOM technique and samples selection

Scanning Near-field Optical Microscopy (SNOM) is a probe microscopy technique for nanostructure investigation capable of ultra-high optical resolution (well below the diffraction limit, $\lambda/2$, of conventional microscopies, as stated in Dunn (1999)). A tapered optical fiber, with an apical radius smaller than 100 nm, is placed in resonant oscillation very close to the sample surface ($\sim$ 1-10 nm) and is used as a local illuminator and collector. The tip is slowly moved (typical time for an image is 30-45 minutes) by piezo motors over the sample reconstructing the morphology and, simultaneously, measuring the optical properties of the surface. In the present study, one or more SNOM reflectivity images have been collected at every wavelength of interest using a configuration illustrated in Fig. 1.

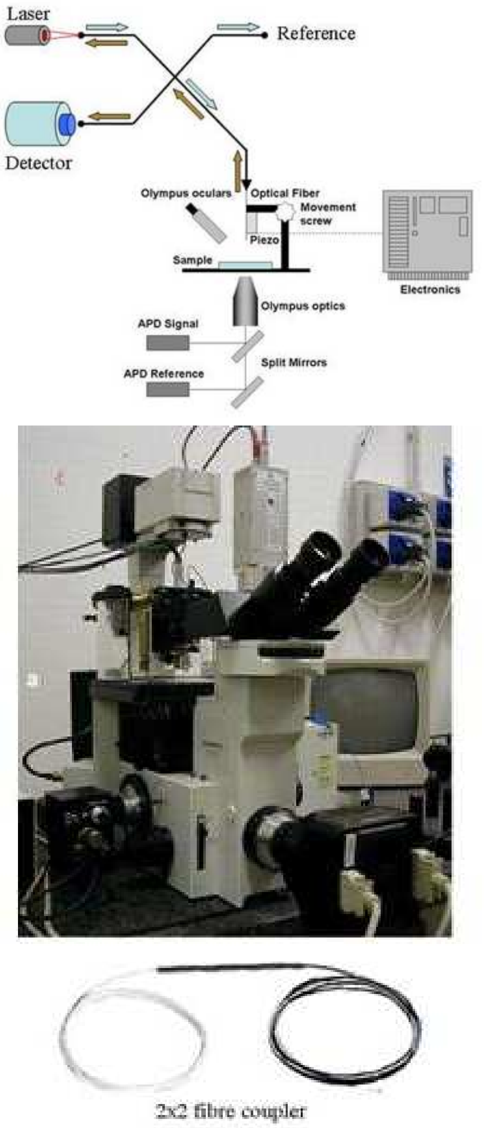

Fig. 1. SNOM instrument and setup. *Up:* Schematic representation. *Down:* Laboratory model picture.

3. Work procedure and preliminary results

This work is the first multi-colour SNOM experiment (i.e. reflected light images of the same sample have been taken at different wavelengths) ever performed on extraterrestrial samples. The wavelengths of interest are contained in the bands of maximum or minimum reflectance of olivine and pyroxenes (476 nm, 516 nm, 904 nm, 1300 nm and 1500 nm), the most important components of asteroid surfaces. In this way, we can, in principle, identify, comparing optical images at different wavelengths, regions of the sample containing these minerals. Otherwise, metallic nanostructures could be present in areas characterised by optical properties not compatible with olivine or pyroxenes and, simultaneously, showing an increasing reflectance at increasing wavelength (i.e. reddening).

3.1. Simulations

SNOM simulations were performed using a software that models the interaction between the electromagnetic wave and the sample, and calculates the electromagnetic field distribution in 3D and the electromagnetic energy transmitted and reflected by the sample, solving Maxwell Equations through a variant of the Finite Integration Technique.

The following structure is considered: a 10 μm long tip (produced by tapering an optical fibre), a 4 μm^2 square sample (forsterite, fayalite or enstatite, with or without little iron spheres) placed 8 nm away from the tip apex, a light source that illuminates the waveguide (optical fibre) and two vacuum layers, located, respectively, above the tip and below the sample, to recoil transmitted and reflected light.

Simulation results show that a quite smooth reflectance spatial distribution (i.e. the optical image) is obtained if no metal is present, while npFe contribute to create reflectance peaks (Fig. 2). As expected, these latter are the stronger when increasing the wavelength: it is found that an iron nanoparticle produces a very intense reflectance peak at 1300 nm and 1500 nm, a small peak at 904 nm and has no influence on the reflectance at 476 nm and 516 nm.

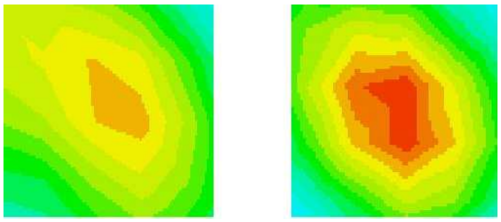

Fig. 2. Simulated distributions of reflected light by a forsterite sample, in absence (left) and in presence (right) of an iron nanoparticle. It can be seen that in the first case distribution is less peaked than in the presence of the nanoparticle.

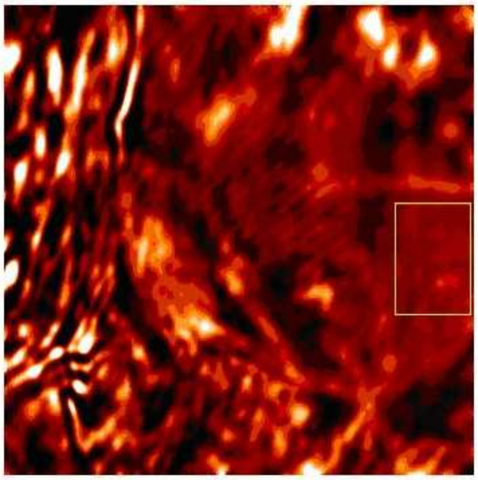

Fig. 3. Optical image at 1500 nm of an analysed sample. The darker the color, the lower the reflectance. The region contained in the white rectangle has been associated to pure silicate, because of its constant reflectance. The region on the left is associated to scatterers that create interference fringes. The elliptic areas above or the rounded ones at the center can be npFe agglomerates.

3.2. Analysis of laboratory images

Images of the same sample collected at different wavelengths have a slight different spatial scale due to small but unavoidable mechanical drift occurring during the data acquisition. Therefore, first operation of data reduction has been to calculate (bi-dimensional) spatial shift between the optical images, applying a cross-correlation analysis on the respective topographies. After a satisfactory image alignment, the presence of metallic inclusions in the samples can be investigated.

A technique of semi-quantitative comparison has been applied for the nanophase detection. Because simulation results show that npFe cause reflectance peaks at the longest wavelengths, the regions of the sample having an uniform reflectance distribution at all the wavelengths have been associated to pure silicates (without metal), while regions having an uniform reflectance distribution at the shorter wavelengths and a peaked reflectance distribution at the longer ones, if not compatible with

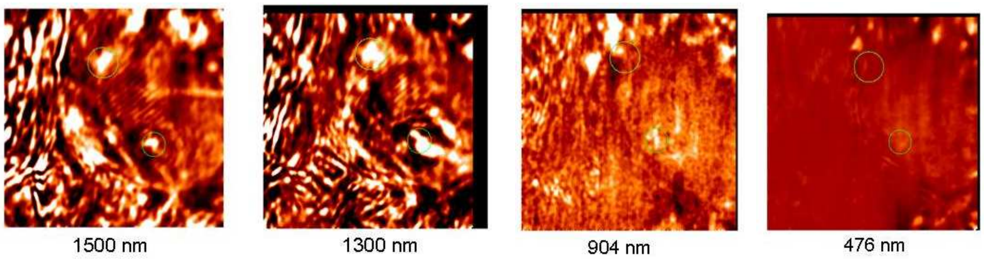

Fig. 4. Reflectance images at different wavelengths. Regions contained in the green circles can host metallic inclusions.

other optical effects, however easily detectable (i.e. interference fringes), could host npFe (Fig. 3)

Once identified a region associated with pure silicate and calculated, for every wavelength, its mean reflectance (hereon R_s) and the corresponding standard deviation (σ), a region of mean reflectance R_i is considered as potentially hosting metallic inclusions if:

- at 1300 nm and 1500 nm $R_i - R_s > 2\sigma$;
- at 904 nm R_i is higher than R_s;
- at 476 nm and 516 nm, R_i is comparable to R_s

4. Conclusions and next steps

Identification of npFe on Ordinary Chondrites samples is developing by means of both simulations techniques and SNOM measurements.

According to simulations, reflected intensity at the longest wavelengths (1300 nm and 1500 nm) has a smoother distribution in pure silicate samples, while, in samples with metallic inclusions, it peaks in correspondence of a npFe. This result has been used to develop a semi-quantitative method to detect npFe in the analysed samples: we assumed that metallic inclusions would cause strong reflectance peaks at the longer wavelengths, while they would be unobserved at the shorter ones (476 nm and 516 nm). Application of this method led to the identification of some regions that are expected to host the iron inclusions. It is important to underline the strongness of multi-colour SNOM analysis (for the first time elaborated on extraterrestrial samples) because npFe identification is possible only by comparing optical images at different wavelength.

In the future, we plan to develop a more quantitative method to better recognize regions hosting iron inclusions. Then, a link between the amount of iron contained in the sample and shock degree of mechanical shock experienced by this latter could be searched: this would confirm the scenario, proposed by Moretti et al. (2005), about npFe formation.

Finally, a comparison with the asteroid spectra can clarify the relation between iron content, shock degree and reddening.

References

Bell, D., Bell, J., Haack, H., & Scott, E. 1992, Abstracts of the LPSC, 123, 167
Dunn, R. 1999, Chem. Rev., 99, 2891
Gaffey, M. 1976, JGR, 81, 905
Moretti, P., Maras, A., Palomba, E., et al. 2005, ApJ, 634, 117
Pieters, C., Taylor, L., Noble, S., et al. 2000, Met. Planet. Sci., 35, 1101
Sasaki, S., Nakamura, K., Hamabe, Y., Kurahashi, E., & Hiro, T. 2001, Nature, 410, 555